Trends and variability of midlatitude stratospheric water vapour deduced from the re-evaluated Boulder balloon series and HALOE

M. Scherer, H. Vömel, S. Fueglistaler, S. J. Oltmans, J. Staehelin

HAL Id: hal-00303131
https://hal.science/hal-00303131

Submitted on 18 Jun 2008

**Atmospheric
Chemistry
and Physics
Discussions**

ACPD

7, 14511–14542, 2007

**Trends and variability
in midlatitude
stratospheric H$_2$O**

M. Scherer et al.

Trends and variability of midlatitude stratospheric water vapour deduced from the re-evaluated Boulder balloon series and HALOE

M. Scherer[1], H. Vömel[2,3], S. Fueglistaler[4], S. J. Oltmans[3], and J. Staehelin[1]

[1]Atmospheric and Climate Science, Eidgenössische Technische Hochschule, Zürich,
Switzerland
[2]Cooperative Institute for Research in Environmental Science, University of Colorado, Boulder,
CO, USA
[3]Global Monitoring Division, Earth System Research Laboratory, NOAA, Boulder, CO, USA
[4]Applied Mathematics and Theoretical Physics, Cambridge University, Cambridge, UK

Correspondence to: S. Fueglistaler (s.fueglistaler@damtp.cam.ac.uk)

Title Page

Abstract	Introduction
Conclusions	References
Tables	Figures

|◀| ▶|

| ◀ | ▶ |

| Back | Close |

Full Screen / Esc

Printer-friendly Version

Interactive Discussion

EGU

Abstract

This paper presents an updated trend analysis of water vapour in the lower midlatitude stratosphere from the Boulder balloon-borne NOAA frostpoint hygrometer measurements and from the Halogen Occulation Experiment (HALOE). Two corrections for instrumental bias are applied to homogenise the frostpoint data series, and a quality assessment of all soundings after 1991 is presented. Linear trend estimates based on the corrected data for the period 1980–2000 are up to 40% lower than previously reported. Vertically resolved trends and variability are calculated with a multi regression analysis including the quasi-biennal oscillation and equivalent latitude as explanatory variables. In the range of 380 to 640 K potential temperature ($\approx$14 to 25 km), the frostpoint data from 1981 to 2006 show positive linear trends between 0.3±0.3 and 0.7±0.1%/yr. The same dataset shows trends between −0.2±0.3 and 1.0±0.3%/yr for the period 1992 to 2005. HALOE data over the same time period suggest negative trends ranging from −1.1±0.2 to −0.1±0.1%/yr. In the lower stratosphere, a rapid drop of water vapour is observed in 2000/2001 with little change since. At higher altitudes, the transition is more gradual, with slowly decreasing concentrations between 2001 and 2007. This pattern is consistent with a change induced by a drop of water concentrations at entry into the stratosphere. Previously noted differences in trends and variability between frostpoint and HALOE remain for the homogenised data. Due to uncertainties in reanalysis temperatures and stratospheric transport combined with uncertainties in observations, no quantitative inference about changes of water entering the stratosphere in the tropics could be made with the mid latitude measurements analysed here.

1 Introduction

Water vapour is important in determining radiative and chemical properties of the stratosphere (Kley et al., 2000). An increase of stratospheric water vapour of 1%

per year has been reported for measurements made in Boulder, Colorado since 1980 (Oltmans and Hofmann, 1995; Oltmans et al., 2000) and, based on a combination of several datasets, for the past half century (Rosenlof et al., 2001). These trends indicate a long-term climate change (Rosenlof et al., 2001) and have implications for the Earth's radiative budget (Forster and Shine, 2002), stratospheric temperature and ozone chemistry (Dvortsov and Solomon, 2001). Uncertainties about future stratospheric H_2O concentration affect the ability to predict the recovery of stratospheric ozone (Weatherhead and Andersen, 2006).

The reason for the observed increase is not clear at present. The photo oxidation of methane is the primary source of water vapour in the stratosphere, and the long-term increase in stratospheric CH_4 can account for 24–34% of an increase of 1%/yr in stratospheric H_2O (Rohs et al., 2006). Interannual variability of the entry value of water vapour into the stratosphere ($[H_2O]_e$) is tightly constrained by tropical tropopause temperatures (Fueglistaler et al., 2005; Fueglistaler and Haynes, 2005). However, the water vapour trend observed by Oltmans et al. (2000) and Rosenlof et al. (2001) is at odds with temperature trends at the tropical tropopause (Zhou et al., 2001; Seidel et al., 2001). The increase of El-Niño Southern Oscillation conditions over the last half century (Scaife et al., 2003), Volcanic eruptions (Joshi and Shine, 2003; Austin et al., 2007) or changes in cloud microphysical properties (Sherwood, 2002; Notholt et al., 2005) may have affected stratospheric water vapour, but clear evidence that any of these processes could account for the magnitude of the observed trend is missing.

Water vapour measurements at stratospheric concentrations (typically a few parts per million) are difficult and require sophisticated techniques. The NOAA ESRL GMD (formerly NOAA CDML) balloon-borne measurements with a frostpoint hygrometer (henceforth termed NOAA FP) is the only available continuous multi-decade record, covering the last 27 years. This series is one of the most often used dataset for stratospheric water vapour; either for comparisons with satellite data and models, or for studies investigating the effect of increasing stratospheric moisture (e.g. Forster and Shine, 2002; Sherwood, 2002; Shindell, 2001; Randel et al., 2001, 2004, 2006; Stenke and

Grewe, 2005; Fueglistaler and Haynes, 2005; Chiou et al., 2006; Austin et al., 2007). However, assessment of trends is complicated by unresolved discrepancies between measurements of different instruments (see Kley et al., 2000). NOAA FP and Halogen Occultation Experiment (HALOE) (Russell et al., 1993) time series show systematic
5   differences for trend estimates (Randel et al., 2004).

Here, we provide a new analysis of the NOAA FP data set and compare it with HALOE data for the period 1992–2005. Section 2 discusses data and bias corrections. The statistical model used to calculate trends and variability is described in Sect. 3, and Sect. 4 presents the results. Section 5 addresses the question whether the midlatitude
10 water vapour measurements provide new insight into processes controlling $[H_2O]_e$. Finally, Sect. 6 summarises our conclusions.

2   Data

2.1   NOAA frostpoint hygrometer

The NOAA FP is a balloon borne instrument based on the chilled-mirror principle. The
15 Clausius-Clapeyron equation is used to determine the vapour pressure over an ice layer which is in equilibrium with the water vapour above. The instrument has been previously described (Oltmans, 1985; Vömel et al., 1995; Oltmans et al., 2000). The overall accuracy for this instrument is about 0.5 K in frostpoint temperature, corresponding to an uncertainty in mixing ratio of about 10% under stratospheric conditions. The
20 balloon soundings typically reach an altitude of 28–30 km. The design of the instrument allows collection of data during ascent and descent. Outgassing of water vapour in the NOAA FP inlet and from the balloon envelope is a source of possible contamination during ascent, but not during descent (when the instrument is ahead of the balloon). Generally, uncontaminated data can be collected up to an altitude of about 25 km. All
25 data before 1991 were manually extracted from a recorder strip chart. From 1991 onwards a digital recording system was implemented together with other new electronics.

Title Page

Abstract | Introduction

Conclusions | References

Tables | Figures

|◄ | ►|

◄ | ►

Back | Close

Full Screen / Esc

Printer-friendly Version

Interactive Discussion

EGU

The dataset used in this study has been significantly revised compared to the dataset used by Oltmans et al. (2000). The next two sections document these changes.

2.1.1 Data corrections

Since the publications of Rosenlof et al. (2001) and Oltmans et al. (2000) two sources of bias in the measurement of the frostpoint temperature were identified. The biases and their corrections are described in detail in Appendix A. Essentially, water vapour measurements prior to 1987 were biased low, whereas those from 1991 onward were biased high. Consequently, the corrected data series yields a linear trend estimate lower than previously published. Figure 1 shows the time series and trend estimates as in Oltmans et al. (2000). Trends for the period 1980–2000 between 14 and 25 km altitude are reduced by up to 40% and range, after the correction, between 0.2 and 1.05%/yr. The reduction in the trend becomes larger with increasing altitude, since the corrections are proportional to the frostpoint temperature, which is decreasing with altitude.

2.1.2 Evaluation of data quality of individual soundings

In order to better understand the disagreement between HALOE and NOAA FP, we evaluated the quality of each NOAA FP profile with respect to the following sources of potential errors. First, in some cases the measured frostpoint temperature exhibits large oscillations caused by the instruments feed-back controller. This is often not considered to be a problem, and data may be processed with a low pass filter (Vömel et al., 2007b). However, excessive oscillations may indicate erroneous data. Second, the comparison of data collected during ascent and descent allows some consistency checks. The aforementioned sources for contamination may lead to larger values during ascent than descent, but systematically lower values during ascent may indicate instrumental problems. Profiles that showed excessive mirror oscillations and/or systematically higher values during descent were flagged as being of lower quality, and

Title Page

Abstract | Introduction

Conclusions | References

Tables | Figures

⏮ | ⏭

◀ | ▶

Back | Close

Full Screen / Esc

Printer-friendly Version

Interactive Discussion

EGU

the subsequent analyses are carried out for both all profiles, as well as for only those of higher quality.

Soundings before 1991 were manually extracted from chart recorder strips which do not allow the type of screening described above. Table 1 provides the number of retrieved soundings in each year together with the number of higher quality soundings. A total of 44 out of 191 soundings were classified to be of lower quality. Unfortunately, in the years just before the observed "drop" in 2001, only a handful of soundings are of higher quality (with consequences for the trend estimates, see below),

Figure 2 shows the time series of measurements averaged in the layers of 380–420 and 580–620 K potential temperature. Generally, the lower quality measurements (green dots) fall well within the range of the higher quality measurements (black dots). However, the 12-month moving averages between the two datasets differ particularly in the years around the year 2000. Despite the newly applied corrections, the previously noted (Randel et al., 2006) sytematic differences to the HALOE measurements (orange dots) remain.

2.2 HALOE

HALOE retrieved profiles of various trace gases (including water vapour) based on solar occultation measurements (with about 15 sunrise and 15 sunset events per day) between September 1991 and November 2005. Measurements on any day were made at about the same latitude, but shifted in longitude. The profiles for water vapour range from about 15 to 80 km altitude and latitudinal coverage was from 60° S to 60° N over the course of one month. The vertical resolution of the instrument is 1.6 km at the limb tangent point, and water vapour concentrations are calculated from extinction measurements at 6.61 micrometers. HALOE (version 19) data for profiles near Boulder, Colorado (within 35°–45° N and 130°–80° W) were obtained from the HALOE website (http://haloedata.larc.nasa.gov/download/index.php). Only data from July 1992 onward were used to minimize errors arising from enhanced stratospheric aerosol loading following the eruption of Mt. Pinatubo in 1991. Figure 2 shows the HALOE measurements

EGU

for the same layers of potential temperature as the NOAA FP measurements. As already noted above, the HALOE and NOAA FP timeseries show systematic differences which will be further quantified below.

3 Statistical modelling

The monthly binned H_2O values Y_t with t denoting the number of months from the start of the time series ($t=1...T$) are represented in general form as

$$Y_t = \mu + X_t + S_t + Z_t + N_t \tag{1}$$

where μ represents a term for constant offset(s). $X_t = \sum_i^n \omega_i X_{i,t}$ represents trend terms with ω_i representing the change per year. S_t is the term for the seasonal cycle represented by the annual components: $S_t = \alpha \sin(2\pi t/12) + \beta \cos(2\pi t/12)$ and Z_t represents the contribution of the proxies (here QBO and Equivalent latitude). The term N_t stands for the unresolved noise. The noise is modelled as an autoregressive process of first order $N_t = N_{t-1} + \epsilon_t$, where ϵ_t are independent random variables with zero mean and a common variance σ_ϵ^2.

The QBO affects tropical tropopause temperatures (Baldwin et al., 2001) and as a consequence the stratospheric entry value of water vapour (Giorgetta and Bengtsson, 1999; Fueglistaler and Haynes, 2005). The influence of the QBO is modelled with a combination of equatorial zonal winds at 30 and 70 hPa (QBO_{30} and QBO_{70}, courtesy of B. Naujokat, FU Berlin):

$$\gamma_{QBO} Z_{QBO,t} = \gamma_{30} QBO_{30,t} + \gamma_{70} QBO_{70,t}, \tag{2}$$

where γ is the coefficient determined by the linear regression for each level. The two wind time series differ by about $\pi/2$ in phase and can therefore automatically adjust a variable time lag (Bojkov and Fioletov, 1995).

We use equivalent latitude (ϕ_{eq}) (Sobel et al., 1997) to account for variability associated with stratospheric waves. Equivalent latitude profiles are calculated based on potential vorticity fields derived from NCEP reanalysis data (Kalnay et al., 1996, obtained from their web site at http://www.cdc.noaa.gov/). More precisely, the proxy is the difference between ϕ_{eq} of the measurement and the latitude of Boulder ($\phi_0 = 40°\,N$)

$$Z_{\phi_{eq},t} = \phi_{eq,t} - \phi_0. \tag{3}$$

Neither the QBO nor the equivalent latitude proxy shows a trend over the periods 1981–2006 or 1992–2005, and cannot contribute to a trend in water vapour of these periods.

A simple linear trend calculation may be obtained from a regression model of the form

$$Y_t = \mu + \omega_1 X_{1,t} +$$
$$S_t + \gamma_{QBO} Z_{QBO,t} + \gamma_{\phi_{eq}} Z_{\phi_{eq},t} + N_t \tag{4}$$

where μ is a constant offset, $X_{1,t} = t/12$ and ω_1 is the trend per year. A better representation of the observations may be obtained with a statistical model that accounts for the drop observed around 2001:

$$Y_t = \mu_1 + \delta\,\mu_2 + \omega_1 X_{1,t} + \omega_2 X_{2,t} +$$
$$S_t + \gamma_{QBO} Z_{QBO,t} + \gamma_{\phi_{eq}} Z_{\phi_{eq},t} + N_t \tag{5}$$

where μ_1 is again a constant offset and μ_2 is

$$\mu_2 = \begin{cases} 0 & t < T^* \\ 1 & t \geq T^* \end{cases} \tag{6}$$

where T^* is the time of the discontinuity δ. $X_{1,t}$ is $t/12$ and $X_{2,t}$ takes the form

$$X_{2,t} = \begin{cases} 0 & t < T^* \\ (t - T^*)/12 & t \geq T^* \end{cases} \tag{7}$$

Trends and variability in midlatitude stratospheric H$_2$O

M. Scherer et al.

EGU

$X_{2,t}$ is 0 up to the date of trend change T^*, and increases linearly after that, so that ω_2 is the departure from the trend ω_1 after T^*. The trend estimator before the date of change T^* is ω_1, after T^* it is $\omega_1 + \omega_2$ (see Reinsel et al. (2002) for details of a regression analysis using a term like $X_{2,t}$). T^* is taken as January 2001.

5   All data is analysed on isentropic surfaces in the range of 380–640 K (i.e. in the stratospheric "overworld" Holton et al., 1995). The analysis for NOAA FP data is made for the periods 1981–2006 and for 1992–2005 (to allow direct comparison with HALOE data). Due to limited data, we refrain from presenting seasonally resolved trends and variability.

10   4   Results: variability and trends

4.1   Variability

The variability of water vapour in the altitude range between 380 K and 640 K ($\approx$14 and 25 km) and the contribution of the proxies to this variability is shown in Figs. 3 and 4. The top panels in Fig. 3 show the variability of the time series (thick line), as well as the

15   residual standard error of the regression model (thin line). We note a clear difference in variability of the layers below and above 450 K. Below 450 K, the variability ranges from 0.4 to 1.4 ppmv for NOAA and from 0.2 to 1.1 ppmv for HALOE. Above 450 K, the variability for NOAA FP is around 0.4 to 0.5 ppmv, and about 0.2 ppmv for HALOE. Thin lines in the top panels of Fig. 3 denote the residual standard error of the regression

20   model.   Below 450 K the seasonal cycle (see Fig. 3c/d) is the dominant source of variation, which is well captured by the statistical model.   However, higher up, the proxies fail to explain most of the observed variability. Variability for the whole NOAA FP dataset (dotted lines) is slightly lower, which may be counter intuitive. However, as noted earlier, the majority of the excluded soundings do not appear to be outliers, such

25   that the variability of the entire dataset is not necessarily larger than that of the higher quality data only.

4.1.1 Seasonal cycle

The amplitude of the seasonal cycle is shown in the lower panels of Fig. 3. The amplitude is calculated as the standard deviation of the proxy time series multiplied with its estimated coefficient, i.e. SD($\alpha \sin \frac{\pi}{6}t + \beta \cos \frac{\pi}{6}t$) is the amplitude of the seasonal component. For the NOAA FP, the amplitude of the annual component is about 1 ppmv at 380 K and decreases linearly to 0.1 ppmv at 450 K. For HALOE, the decay of the amplitude of seasonal variability is slightly smoother, but both measurements reveal a change in circulation and transport around 450 K (roughly the base of the "tropical pipe" Plumb, 1996).

4.1.2 QBO and equivalent latitude

The vertically resolved variability accounted for by the QBO and ϕ_{eq} is shown in Fig. 4. The amplitude of the QBO component in the NOAA FP data is about 0.1 ppmv. Over much of the profile, the values are statistically not significant at the 2-σ level. HALOE shows similar amplitudes for the QBO component, but a different shape of the profile (values between 450 and 600 K are significant).

Similar to the QBO, the amplitudes of ϕ_{eq} are small (less than 0.1 ppmv) in both NOAA FP and HALOE data. Again, the shape of the profiles differs somewhat, but given the minor role played by these proxies, further analysis of these differences is not warranted.

4.2 Linear trends

Linear trends derived from Eq. 4 are shown in Fig. 5. The trend estimates based on NOAA FP (higher quality) data for the period 1981–2006 show trends (with their 2-σ uncertainties) ranging from 0.012±0.005 to 0.031±0.005 ppmv/yr, which are significant over most of the altitude range. For the period 1992–2005, the NOAA FP trends are not significant below about 500 K. For both periods, the trends based on all NOAA

Title Page

Abstract | Introduction

Conclusions | References

Tables | Figures

◄◄ | ►►

◄ | ►

Back | Close

Full Screen / Esc

Printer-friendly Version

Interactive Discussion

EGU

FP profiles are generally higher than those based on the higher quality profiles only. In contrast to the NOAA FP data, HALOE data suggest negative trends that peak at 420 K with −0.04±0.02 ppmv/yr, but the tendency towards more positive trends with height is similar to that found in the NOAA FP data.

5   4.3   Decrease in 2001

Global mean deseasonalised water vapour anomalies from HALOE (at 82 hPa) show a rather fast decrease at the beginning of 2001 (Randel et al., 2006). Linear trends from 1981–2006, and for the shorter period 1992–2005, with no distinction between the periods before and after 2001, may not provide an appropriate description of the
10 changes in stratospheric water vapour. Hence we use a regression model as described in Eq. (5), which calculates trends before and after 2001 separately. Figure 6 shows observations and regression fit together with the trend estimates for both periods. For the layer 380–420 K, the model yields slightly increasing water vapour concentrations before and after 2001, and a drop of 0.2±0.6 ppmv and 0.45±0.0008 ppmv for NOAA
15 FP and HALOE, respectively. For the layer 580–620 K, both NOAA FP and HALOE show positive trends before 2001, and negative trends afterwards. In this layer, the change in 2001 is a decrease of −0.13±1.12 ppmv for NOAA FP, whereas the fit to the HALOE data gives actually a small 0.04 ± 0.08 ppmv increase.

    The magnitude and significance of trends and discontinuities differ between NOAA
20 FP and HALOE. The drop, which is clearly seen in the HALOE data at the lower level, is not significant for NOAA FP data at the 2 σ-level. Nevertheless, the main features of the fit and its difference between the two altitudes is similar for both datasets. Water vapour concentrations at higher altitudes show a smoother turnaround compared to the sharp drop at lower altitudes. This difference can be attributed to the broader distribution of
25 age of air (see e.g. Waugh and Hall, 2002) at higher altitude.

    These results suggest hat the observed decrease is really a "drop" rather than a "trend reversal". At present, H_2O in the stratosphere below ≈450 K does not appear to decrease further after 2001. In fact, the linear trend estimates suggest an increase

Trends and variability in midlatitude stratospheric H_2O

M. Scherer et al.

EGU

since 2001 of similar order to that before 2001. However, both trend estimates are based on relatively short periods that leads to large uncertainties (particularly for the period 2001–2005). The exact magnitude of the trends thus depends also to some extent on the "start/end time" of the time series.

Because many NOAA FP profiles in the years before the drop were rated as being of lower quality, the trend estimates based on all NOAA FP profiles yield different results. Figure 7 shows the time series of deseasonalized water vapour anomalies of the layer 380-420 K for all (yellow) and the high quality (green) NOAA FP measurements, and those from HALOE (red). Compared to the higher quality data set, trends calculated with all NOAA FP measurements (not shown) are more positive for the period before 2001, and more negative after 2001. Also, the drop in 2001 is larger.

5 Discussion of the long-term trend

Variability and trends in stratospheric water vapour over Boulder may be caused by changes in the fraction of oxidised methane (which depends mainly on the "age of air" distribution), and changes in the entry mixing ratios of methane and water vapour. Of particular interest is the question whether observations suggest a long-term trend in the water vapour entry mixing ratios, which could indicate important changes in transport of water, and possibly other trace gas species, into the stratospheric overworld. More specifically, the question is whether stratospheric water vapour shows variations and trends that cannot be explained by temperature variations in the vicinity of the tropopause.

Here, we use a simple model to predict water vapour mixing ratios over Boulder based on water vapour and methane entry mixing ratios. Due to relatively short time series and the low number of NOAA FP profiles, we use a simple forward model as previously used by Fueglistaler and Haynes (2005) instead of a regression analysis. (Results and conclusions obtained from a regression analysis were very similar to those presented below.)

5.1 Model

Following Fueglistaler and Haynes (2005) we write water vapour in the stratospheric overworld ($[H_2O]_o$) as

$$[H_2O]_o = [H_2O]_{CH_4} + [H_2O]_{[H_2O]_e} \qquad (8)$$

The contribution of the methane oxidation to H_2O at a given altitude is

$$[H_2O]_{CH_4}(\theta, t) = \alpha([CH_4]_e(t - \tau(\theta)) - [CH_4](\theta, t)) \qquad (9)$$

where α is ≈ 2 (Le Texier et al., 1988). $[CH_4]_e$ is a 2nd order polynomial fit to tropospheric global mean CH_4 (see Dlugokencky et al. (2003) and references therein) and $[CH_4]$ is a 2nd order fit to stratospheric CH_4 measurements at midlatitudes (Rohs et al., 2006). τ is the mean age of midlatitude stratospheric air. Midlatitude stratospheric water vapour that can be accounted for by $[H_2O]_e$ is obtained from

$$[H_2O]_{[H_2O]_e}(\theta, t) = \int_0^6 [H_2O]_e(t - \tau) \cdot w(t - \tau) \cdot h(\theta, \tau) \, d\tau \qquad (10)$$

where $w(t-\tau)$ is a weighting function accounting for the seasonally varying troposphere to stratosphere upward mass flux in the tropics (Holton, 1990). $h(\tau)$ are midlatitude age spectra of stratospheric air truncated at 6 years which were obtained from Andrews et al. (2001) and from Waugh and Hall (2002).

We restrict the timeseries of water vapour entry mixing ratios given by Fueglistaler and Haynes (2005) to the period where ERA-40 (tropical tropopause) temperatures do not show larger deviations (that is, about a 1 K drift over a 5 year period) from radiosonde measurements. As a test of the self consistency of the model and water vapour observations, we also analyse results obtained from a calculation where we replace $[H_2O]_e$ in Eq. (10) with tropical (30° S–30° N) H_2O at 400 K as measured by HALOE ($[H_2O]_{400}$).

EGU

5.2   Results

Figure 8 shows observations (green for NOAA FP, orange for HALOE) and model predictions (black, red for the model based on HALOE $[H_2O]_{400}$) for the layers of 410–450 K, 440–480 K and 600–620 K. Generally, the model yields better agreement with HALOE than with NOAA FP for all levels. The model predictions based on HALOE tropical measurements are very similar to those based on ERA-40 circulation and temperature presented by Fueglistaler and Haynes (2005). However, we note that the model predictions tend to systematically overestimate/underestimate observations at the beginning/end of the timeseries.

Figure 9 shows the differences between the model predictions and the observations with a linear trend fit. The magnitude of the residual trend between model prediction and NOAA FP is larger than the trend in the residual between the model prediction and HALOE data. At 410–450 K, for the NOAA FP the trend in the residual is 0.073±0.016 ppmv/yr, and at 600–640 K it is 0.091±0.017 ppmv/yr. For the HALOE data, the trends in the residual for these layers are 0.021±0.08 ppmv/year and 0.044±0.044 ppmv/yr. The predictions based on HALOE tropical measurements yield a trend in the residual with a magnitude that tends to be smaller than that of the model predictions for entry mixing ratios (but note that we cannot calculate the trends for the same periods).

The fact that the model predictions based on HALOE tropical measurements do not give perfect agreement with the HALOE measurements over Boulder may indicate that the age spectrum, and hence the fraction of oxidised methane does not remain constant. It has been suggested that the stratospheric circulation increases with increasing greenhouse gas concentrations (e.g. Butchart and Scaife, 2001, Austin and Li, 2006), but its impact over the short periods considered here is presumably marginal.

The fact that the sign of the residual trend is the same for both HALOE and NOAA FP may be seen as an indicator that the $[H_2O]_e$ timeseries has a systematic trend bias. When converted to temperature, that bias is of order 2 K/decade for the NOAA

Title Page

Abstract | Introduction

Conclusions | References

Tables | Figures

◄◄ | ►►

◄ | ►

Back | Close

Full Screen / Esc

Printer-friendly Version

Interactive Discussion

EGU

FP measurements, and less than 1 K/decade for the HALOE measurements. In order to quantify a trend in $[H_2O]_e$ that is not controlled by the processes considered by Fueglistaler and Haynes (2005), one would need (i) time series of observations from different instruments that yield consistent trend estimates, and (ii) a reanalysis dataset with residual trends in tropopause temperatures that are much smaller than 1 K/decade. Clearly, the ERA-40 temperatures do not satisfy this requirement.

6 Conclusions

We have presented an analysis of the NOAA FP water vapour measurements in the stratospheric overworld over Boulder, Colorado. We have applied two corrections for newly identifed biases in the measurements, and quality-screened all observations. The corrected measurements show linear trends that are up to 40% smaller than those previously published. For the period 1980–2000, the new linear trend estimates are 0.33±0.05 ppmv/yr for 18–20 Km, and 0.027±0.006 ppmv/yr for 24–26 Km. Previously noted systematic differences (larger variability, larger linear trends) to HALOE remain for the corrected NOAA FP data.

Analysis with a statistical model showed that most of the variability is associated with seasonal variations, and that the QBO and equivalent latitude play only a minor role. Similar to HALOE, the NOAA FP data show a sudden drop of water vapour concentrations at the base of the stratospheric overworld, where rapid quasi-isentropic transport ensures fast communication of changes in water vapour entry mixing ratios to the middle latitudes. Consequently, a linear trend fit over the period 1980–2006 may not be fully appropriate, and we have used a statistical model that accounts for the trend discontinuity in 2001. The statistical model for the layer 380–420 K yields positive linear trends of 0.027±0.031 ppmv/yr for the period 1992–2001, 0.016±0.066 ppmv/yr for the period 2001–2006, and a drop of −0.2±0.6 ppmv in 2001. Water vapour concentrations thus tend to increase over both periods when viewed separately, albeit the trends have very large uncertainty. Higher up in the stratosphere, the discontinuity in

EGU

Printer-friendly Version

Interactive Discussion

EGU

entry mixing ratios is masked by the broad age spectrum of air masses that acts as a low-pass filter. The observed pattern of changes in water vapour concentrations indicates that the change arises from processes that affect water vapour concentrations at entry into the stratosphere, and we emphasize that the water vapour timeseries shows a discontinuity rather than a "trend reversal". The observed discontinuity as well as the substantial reduction of linear trend estimates indicate that great caution should be used with respect to predictions of the impact of stratospheric water vapour on radiative forcing and stratospheric temperature and ozone in the coming decades.

We have tried to quantify a residual trend in stratospheric water vapour entry mixing ratios from the difference between NOAA FP and HALOE middle latitude measurements to values predicted from a simple model. The model assumes constant age of air over time, and [H$_2$O]$_e$ is based on large scale temperatures and circulation in the vicinity of the tropical tropopause (Fueglistaler and Haynes, 2005). The residual trends (observation minus model) are much larger for NOAA FP than HALOE, but are positive for both datasets.

A reliable quantification of trends in [H$_2$O]$_e$ from the NOAA FP and HALOE middle latitude measurements due to processes not considered by Fueglistaler and Haynes (2005) is currently not possible due to the large difference between the residual to NOAA FP and to HALOE data. Moreover, the model predictions of [H$_2$O]$_e$ would require a reanalysis data set with erroneous drifts in tropical tropopause temperatures that are substantially smaller than 1 K/decade; a requirement currently not fulfillled by either ERA-40 or the NCEP reanalyses. Our analysis demonstrates the need for ongoing efforts to obtain long and continous time series of stratospheric water vapour.

Appendix A

Details of hygrometer corrections

Two instrumental sources of bias have been identified for the NOAA FP, which have not previously been applied to all of the data. The first bias is due the calibration of the thermistor, which measures the mirror temperature that is reported as frostpoint temperature. All thermistors are calibrated at three fixed temperatures ($0°C$, $-45°C$ and $-79°C$). A model fit (Layton, 1961) based on the resistance at these three temperatures, is used to describe the relationship between resistance and mirror-temperature. An extended calibration over the temperature range from $-100°C$ to $+20°C$ has shown differences between the modelled and the actual temperature (Vömel et al., 2007b). For temperatures below -79° C the difference between model and real temperature becomes increasingly significant, with a warm bias reaching $0.16°C$ at a frostpoint temperature of $-90.0°C$. The Naval Research Laboratory (NRL) handbook included a linear correction ($T_{\text{fp,corr}} = 1.013245\,T_{\text{fp}} + 1.0464$) for frostpoint temperatures below $-79°$ C, based on a few measurements at $-94.3°C$. This correction has been applied to the data prior to 1991, but not afterwards. The following correction, based on the new calibration has been applied to the post 1990 dataset for frostpoint temperatures below $-79°C$ (T_{fp} in $°C$)

$$T_{\text{fp,corr}} = T_{\text{fp}} - (-0.029(T_{\text{fp}} + 79) + 0.083)^2 \qquad \text{(A1)}$$

The difference between this and the linear NRL correction is, for the relevant temperatures, about a factor of 30 smaller than the total uncertainty of the measurement so that the data before 1991 have not been reprocessed to homogenise this correction.

A second issue is the self-heating of the thermistors in the calibration setup used prior to 1987. The multi-meter current used to read the thermistor resistance at $0°C$ was too large and caused significant self-heating, resulting in a roughly $1.5°C$ warm bias at the $0°C$ calibration point. The model fit propagates this bias at $0°C$ to all other

EGU

temperatures (except for the -45°C and -79°C calibration points), which leads to a cold bias of up to 0.21° C at -90°C. In order to account for the self-heating, the following empirical function has been applied to all data prior to 1987, again only for frostpoint temperatures of -79°C and lower (T_{fp} in $^\circ$C).

$$T_{\text{fp,corr}} = T_{\text{fp}} + (0.0203(T_{\text{fp}} + 61.9))^2 - 0.119 \tag{A2}$$

Acknowledgements. We would like to thank J. Harris, E. Weatherhead and K. Rosenlof for discussions during the course of this work.

References

Andrews, A. E., Boering, K. A., Wofsy, S. C., Daube, B. C., Jones, D. B., Alex, S., Loewenstein, M., Podolske, J. R., and Strahan, S. E.: Empirical age spectra for the midlatitude lower stratosphere from in situ observations of CO$_2$: Quantitative evidence for a subtropical "barrier" to horizontal transport, J. Geophys. Res., 106, 10 257–10 274, doi:10.1029/2000JD900703, 2001. 14523

Austin, J. and Li, F.: On the relationship between the strength of the Brewer-Dobson circulation and the age of stratospheric air, Geophys. Res. Lett., 33, L17807, doi:10.1029/2006GL026867, 2006. 14524

Austin, J., Wilson, J., Feng, L., and Vömel, H.: Evolution of water vapor concentrations and stratsophereic age of air in coupled chemistry-climate model simulations, J. Atmos. Sci., 64, 905–921, doi:10.1175/JAS3866.1, 2007. 14513, 14514

Baldwin, M. P., Gray, L. J., Dunkerton, T. J., Hamilton, K., Haynes, P. H., Randel, W. J., Holton, J. R., Alexander, M. J., Hirota, I., Horinouchi, T., Jones, D. B. A., Kinnersley, J. S., Marquardt, C., Sato, K., and Takahashi, M.: The quasi-biennial oscillation, Rev. Geophys., 39, 179–230, doi:10.1029/1999RG000073, 2001. 14517

Bojkov, R. D. and Fioletov, V. E.: Estimating the global ozone characteristics during the last 30 years, J. Geophys. Res., 100, 16 537–16 552, doi:10.1029/95JD00692, 1995. 14517

Butchart, N. and Scaife, A. A.: Removal of chlorofluorocarbons by increased mass exchange between the stratosphere and troposphere in a changing climate, Nature, 410, 799–802, 2001. 14524

Chiou, E. W., Thomason, L. W., and Chu, W. P.: Variability of Stratosphereric Water Vapor Inferred from SAGE II, HALOE, and Boulder (Colorado) Balloon Measurements, J. Climate, 4121–4133, doi:10.1175/JCLI3841.1, 2006. 14514

Dlugokencky, E. J., Houweling, S., Bruhwiler, L., Masarie, K. A., Lang, P. M., Miller, J. B., and Tans, P. P.: Atmospheric methane levels off: Temporary pause or a new steady-state?, Geophys. Res. Lett., 30, 1992, doi:10.1029/2003GL018126, 2003. 14523

Dvortsov, V. L. and Solomon, S.: Response of the stratospheric temperatures and ozone to past and future increases in stratospheric humidity, J. Geophys. Res., 106, 7505–7514, doi: 10.1029/2000JD900637, 2001. 14513

Forster, P. M. d. F. and Shine, K. P.: Assessing the climate impact of trends in stratospheric water vapor, Geophys. Res. Lett., 29, 10–1, 2002. 14513

Fueglistaler, S. and Haynes, P. H.: Control of interannual and longer-term variability of stratospheric water vapor, J. Geophys. Res., 110, D24108, doi:10.1029/2005JD006019, 2005. 14513, 14514, 14517, 14522, 14523, 14524, 14525, 14526, 14542

Fueglistaler, S., Bonazzola, M., Haynes, P. H., and Peter, T.: Stratospheric water vapor predicted from the Lagrangian temperature history of air entering the stratosphere in the tropics, J. Geophys. Res., 110, D08 107, doi:10.1029/2004JD005516, 2005. 14513

Giorgetta, M. A. and Bengtsson, L.: Potential role of the quasi-biennial oscillation in the stratosphere-troposphere exchange as found in water vapor in general circulation model experiments, J. Geophys. Res., 104, 6003–6020, doi:10.1029/1998JD200112, 1999. 14517

Holton, J. R.: On the Global Exchange of Mass between the Stratosphere and Troposphere., J. Atmos. Sci., 47, 392–396, 1990. 14523

Holton, J. R., Haynes, P. H., McIntyre, M. E., Douglass, A. R., Rood, R. B., and Pfister, L.: Stratosphere-troposphere exchange, Rev. Geophys., 33, 403–439, 1995. 14519

Joshi, M. M. and Shine, K. P.: A GCM Study of Volcanic Eruptions as a Cause of Increased Stratospheric Water Vapor., J. Clim., 16, 3525–3534, 2003. 14513

Kalnay, E., Kanamitsu, M., Kistler, R., Collins, W., Deaven, D., Gandin, L., Iredell, M., Saha, S., White, G., Woollen, J., Zhu, Y., Leetmaa, A., Reynolds, B., Chelliah, M., Ebisuzaki, W., Higgins, W., Janowiak, J., Mo, K. C., Ropelewski, C., Wang, J., Jenne, R., and Joseph, D.: The NCEP/NCAR 40-Year Reanalysis Project., B. Am. Meteorol. Soc., 77, 437–472, 1996. 14518

Kley, D., Russell III, J. M., and Philips, C., eds.: SPARC assessment of upper tropospheric and stratospheric water vapour, WCRP 113, WMO/TD No. 1043, SPARC Report Nr.2, World

Title Page	
Abstract	Introduction
Conclusions	References
Tables	Figures
◀◀	▶▶
◀	▶
Back	Close
Full Screen / Esc	
Printer-friendly Version	
Interactive Discussion	

EGU

Meteorol. Organ., 2000. 14512, 14514

Layton, E. C.: Report of the determination of exactness of fit of thermistor to the equations $\log R = A + B/(T + \Theta)$ and $\log R = A + B/(T + \Theta) + CT$, Tech. Rep. 2168, U.S. Army Signal Res. and Dev. Lab, 1961. 14527

5 Le Texier, H., Solomon, S., and Garcia, R. R.: The role of molecular hydrogen and methane oxidation in the water vapour budget of the stratosphere, Q. J. Roy. Meteorol. Soc., 114, 281–295, 1988. 14523

Notholt, J., Luo, B. P., Fueglistaler, S., Weisenstein, D., Rex, M., Lawrence, M. G., Bingemer, H., Wohltmann, I., Corti, T., Warneke, T., von Kuhlmann, R., and Peter, T.: Influence of tropospheric SO_2 emissions on particle formation and the stratospheric humidity, Geophys.
10 Res. Lett., 32, L07810, doi:10.1029/2004GL022159, 2005. 14513

Oltmans, S. J.: Measurements of water vapor in the stratosphere with a frost point hygrometer, Measurement and Control in Science and Industry, in: Proceedings of the 1985 International Symposium on Moisture and Humidity, pp. 251–258, Instrument Society of America,
15 Washington, D. C., 1985. 14514

Oltmans, S. J. and Hofmann, D. J.: Increase in lower-stratospheric water vapour at a midlatitude Northern Hemisphere site from 1981 to 1994, Nature, 374, 146–149, 1995. 14513

Oltmans, S. J., Vömel, H., Hofmann, D. J., Rosenlof, K. H., and Kley, D.: The increase in stratospheric water vapor from balloonborne, frostpoint hygrometer measurements at
20 Washington, D.C., and Boulder, Colorado, Geophys. Res. Lett., 27, 3453–3456, doi:10.1029/2000GL012133, 2000. 14513, 14514, 14515, 14534

Plumb, R. A.: A "tropical pipe" model of stratospheric transport, J. Geophys. Res., 101, 3957–3972, doi:10.1029/95JD03002, 1996. 14520

Randel, W. J., Zawodny, J. M., and Oltmans, S. J.: Seasonal variation of water vapor in the
25 lower stratosphere observed in Halogen Occultation Experiment data, J. Geophys. Res., 106, 14 313–14 326, doi:10.1029/2001JD900048, 2001. 14513

Randel, W. J., Wu, F., Oltmans, S. J., Rosenlof, K., and Nedoluha, G. E.: Interannual Changes of Stratospheric Water Vapor and Correlations with Tropical Tropopause Temperatures., J. Atmos. Sci., 61, 2133–2148, 2004. 14513, 14514

30 Randel, W. J., Wu, F., Vömel, H., Nedoluha, G. E., and Forster, P.: Decreases in stratospheric water vapor after 2001: Links to changes in the tropical tropopause and the Brewer-Dobson circulation, J. Geophys. Res., 111, D12312, doi:10.1029/2005JD006744, 2006. 14513, 14516, 14521

Title Page	
Abstract	Introduction
Conclusions	References
Tables	Figures

◄◄	►►
◄	►
Back	Close

Full Screen / Esc

Printer-friendly Version

Interactive Discussion

EGU

Reinsel, G. C., Weatherhead, E., Tiao, G. C., Miller, A. J., Nagatani, R. M., Wuebbles, D. J., and Flynn, L. E.: On detection of turnaround and recovery in trend for ozone, J. Geophys. Res., 107, n.a., doi:10.1029/2001JD000500, 2002. 14519

Rohs, S., Schiller, C., Riese, M., Engel, A., Schmidt, U., Wetter, T., Levin, I., Nakazawa, T., and Aoki, S.: Long-term changes of methane and hydrogen in the stratosphere in the period 1978-2003 and their impact on the abundance of stratospheric water vapor, J. Geophys. Res., 111, D14315, doi:10.1029/2005JD006877, 2006. 14513, 14523

Rosenlof, K. H., Chiou, E.-W., Chu, W. P., Johnson, D. G., Kelly, K. K., Michelsen, H. A., Nedoluha, G. E., Remsberg, E. E., Toon, G. C., and McCormick, M. P.: Stratospheric water vapor increases over the past half-century, Geophys. Res. Lett., 28, 1195–1198, doi: 10.1029/2000GL012502, 2001. 14513, 14515

Russell, III, J. M., Gordley, L. L., Park, J. H., Drayson, S. R., Hesketh, W. D., Cicerone, R. J., Tuck, A. F., Frederick, J. E., Harries, J. E., and Crutzen, P. J.: The Halogen Occultation Experiment, J. Geophys. Res., 98, 10 777–10 797, 1993. 14514

Scaife, A. A., Butchart, N., Jackson, D. R., and Swinbank, R.: Can changes in ENSO activity help to explain increasing stratospheric water vapor?, Geophys. Res. Lett., 30, 1880, doi:10.1029/2003GL017591, 2003. 14513

Seidel, D. J., Ross, R. J., Angell, J. K., and Reid, G. C.: Climatological characteristics of the tropical tropopause as revealed by radiosondes, J. Geophys. Res., 106, 7857–7878, doi: 10.1029/2000JD900837, 2001. 14513

Sherwood, S.: A Microphysical Connection Among Biomass Burning, Cumulus Clouds, and Stratospheric Moisture, Science, 295, 1272–1275, doi:10.1126/science.1065080, 2002. 14513

Shindell, D. T.: Climate and ozone response to increased stratospheric water vapor, Geophys. Res. Lett., 28, 1551–1554, doi:10.1029/1999GL011197, 2001. 14513

Sobel, A. H., Plumb, R. A., and Waugh, D. W.: Methods of Calculating Transport across the Polar Vortex Edge., J. Atmos. Sci., 54, 2241–2260, 1997. 14518

Stenke, A. and Grewe, V.: Simulation of stratospheric water vapor trends: impact on stratospheric ozone chemistry, Atmos. Chem. Phys., 5, 1257–1272, 2005, http://www.atmos-chem-phys.net/5/1257/2005/. 14513

Vömel, H., Oltmans, S. J., Hofmann, D. J., Deshler, T., and Rosen, J. M.: The evolution of the dehydration in the Antarctic stratospheric vortex, J. Geophys. Res., 100, 13 919–13 926, doi:10.1029/95JD01000, 1995. 14514

Trends and variability in midlatitude stratospheric H_2O

M. Scherer et al.

Title Page

Abstract	Introduction
Conclusions	References
Tables	Figures

⏮ | ⏭

◄ | ►

Back | Close

Full Screen / Esc

Printer-friendly Version

Interactive Discussion

EGU

Vömel, H., David, D. E., and Smith, K.: Accuracy of tropospheric and stratospheric water vapor measurements by the cryogenic frost point hygrometer: Instrumental details and observations, J. Geophys. Res., 112, D08305, doi:10.1029/2006JD007224, 2007a. 14533

Vömel, H., Yushkov, V., Khaykin, S., Korshunov, L., Kyrö, E., and Kivi, R.: Intercomparison of stratospheric water vapor sensors: FLASH-b and NOAA/CMDL frost point hygrometer, J. Atmos. Ocean. Tech., 27, 941–952, doi:10.1175/JTECH2007.1, 2007b. 14515, 14527

Waugh, D. and Hall, T.: Age of stratospheric air: theory, observations, and models, Rev. Geophys., 40, 1–1, doi:10.1029/2000RG000101, 2002. 14521, 14523

Weatherhead, E. C. and Andersen, S. B.: The search for signs of recovery of the ozone layer, Nature, 441, 39–45, 2006. 14513

Zhou, X.-L., Geller, M. A., and Zhang, M.: Cooling trend of the tropical cold point tropopause temperatures and its implications, J. Geophys. Res., 106, 1511–1522, doi: 10.1029/2000JD900472, 2001. 14513

Trends and variability in midlatitude stratospheric H$_2$O

M. Scherer et al.

Title Page

Abstract | Introduction

Conclusions | References

Tables | Figures

|◄ | ►|

◄ | ►

Back | Close

Full Screen / Esc

Printer-friendly Version

Interactive Discussion

EGU

Table 1. The number of NOAA FP soundings by year. For the years 1991 to 2006 the total number is given (All) as well as the number of higher quality soundings (HQ). The high number of measurements in 2005 is a result of the development of the new Cryogenic Frostpoint Hygrometer (CFH) at the University of Colorado (Vömel et al., 2007a).

	1980	1981	1982	1983	1984	1985	1986	1987	1988	1989	1990
All	1	11	6	9	10	6	10	7	12	12	9

	1991	1992	1993	1994	1995	1996	1997	1998	1999	2000	2001	2002	2003	2004	2005	2006
All	10	11	13	12	13	13	4	9	9	8	8	9	8	18	30	16
HQ	9	10	12	8	12	10	1	1	6	1	8	8	5	16	26	14

EGU

EGU
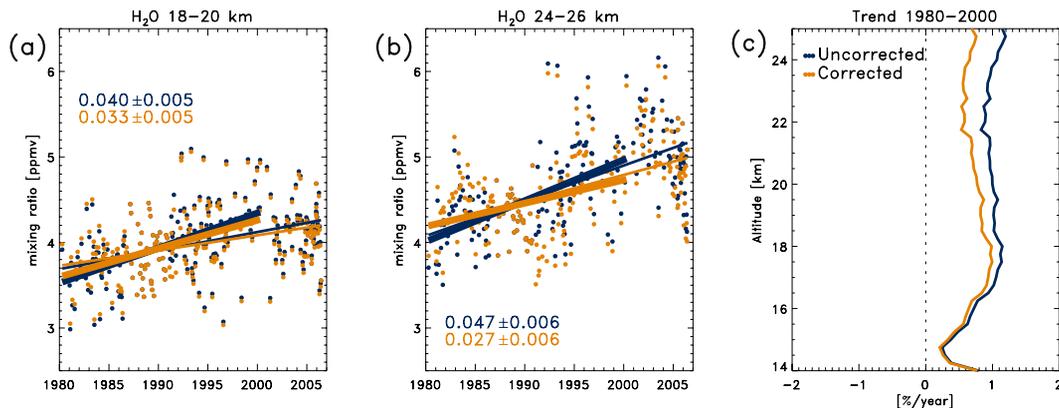
Fig. 1. Linear trend estimates of stratospheric water vapour from NOAA FP measurements. **(a)** For 18–20 Km; **(b)** for 24–26 Km; **(c)** trend profiles (in percent per year, confidence intervals omitted for clarity). Blue/yellow show uncorrected/corrected data, no correction applied for period 1987–1991. Trends for period 1980–2000 (slope and 2-σ uncertainty printed in panels a/b) for comparison with Oltmans et al. (2000). Note trend reduction of up to 40% due to data correction.

EGU
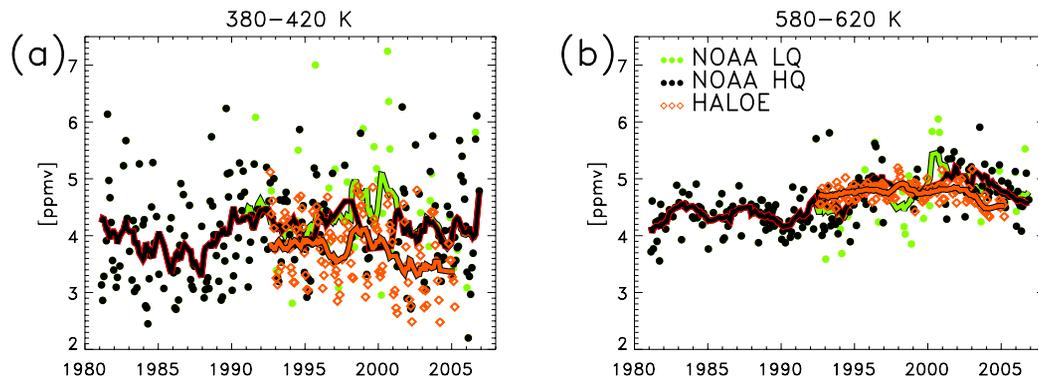
Fig. 2. Water vapour measurements averaged over **(a)** 380–420 K and **(b)** 580–620 K. Black/green: higher/lower quality NOAA FP data; orange: HALOE. Curves show 12 month running mean average (green curve based on all NOAA FP data).
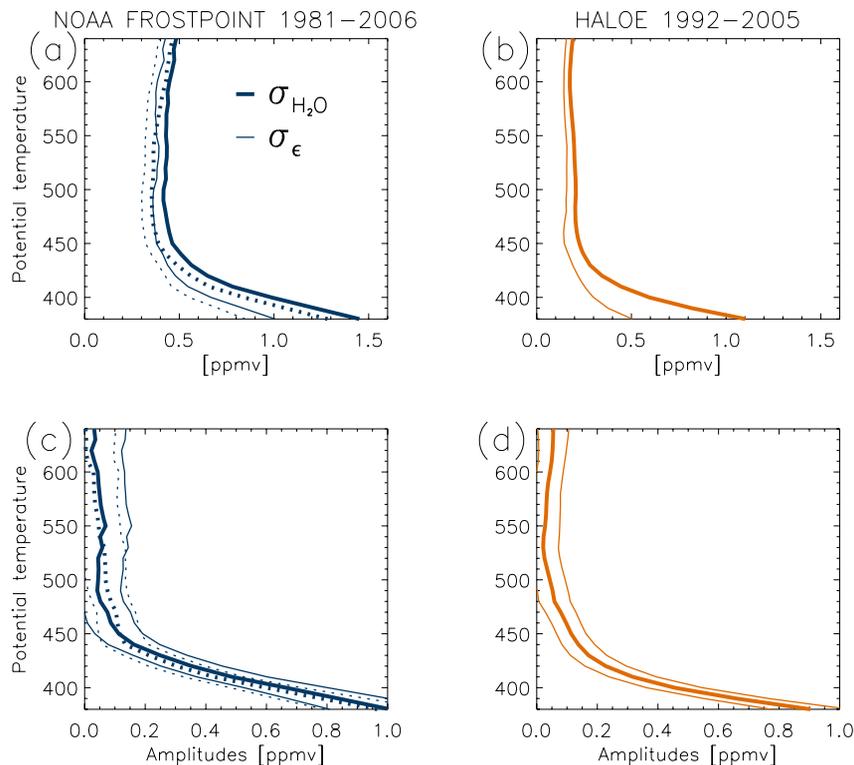
Fig. 3. Standard deviation in the water vapour time series (σ_{H_2O}, thick) and the residuals standard error of the regression model (σ_ϵ, thin) as a function of potential temperature using the regression model in Eq. (4) for **(a)** NOAA FP data from 1981–2006 (dashed lines for all profiles, solid line for higher quality profiles only, see text) and **(b)** HALOE data from 1992–2005. Panels (c,d) show corresponding amplitude of the seasonal cycle (thick lines) and the 2-σ confidence interval (thin lines).

Title Page

Abstract | Introduction

Conclusions | References

Tables | Figures

|◀ | ▶|

◀ | ▶

Back | Close

Full Screen / Esc

Printer-friendly Version

Interactive Discussion

EGU
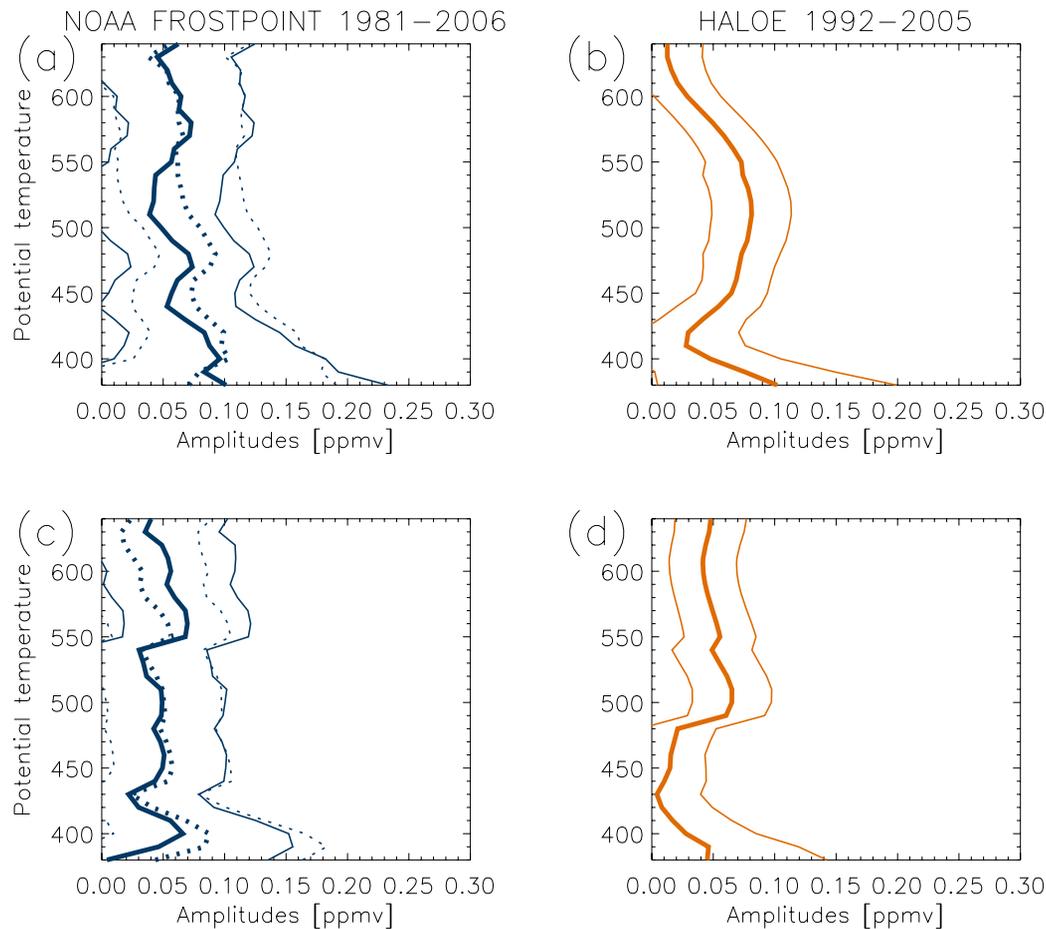
Fig. 4. Amplitude of the QBO proxy for **(a)** NOAA FP and **(b)** HALOE, and amplitude of equivalent latitude for **(c)** NOAA FP and **(d)** HALOE. Same conventions for colors/linestyles as in Fig. 3.
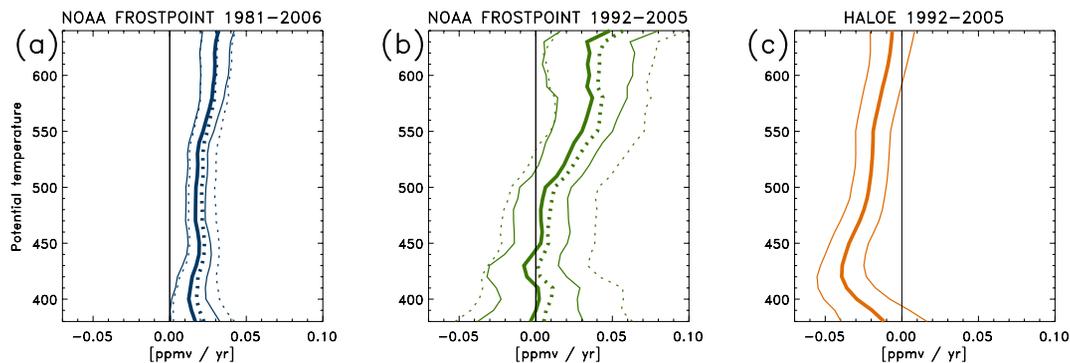
Fig. 5. Trends (thick lines) with the 2-σ confidence intervals (thin lines) calculated with Eq. (4) for **(a)** NOAA FP 1981–2000; **(b)** NOAA FP 1992–2005; **(c)** HALOE 1992–2005. Same conventions for color/linestyles as in Fig. 3.

EGU
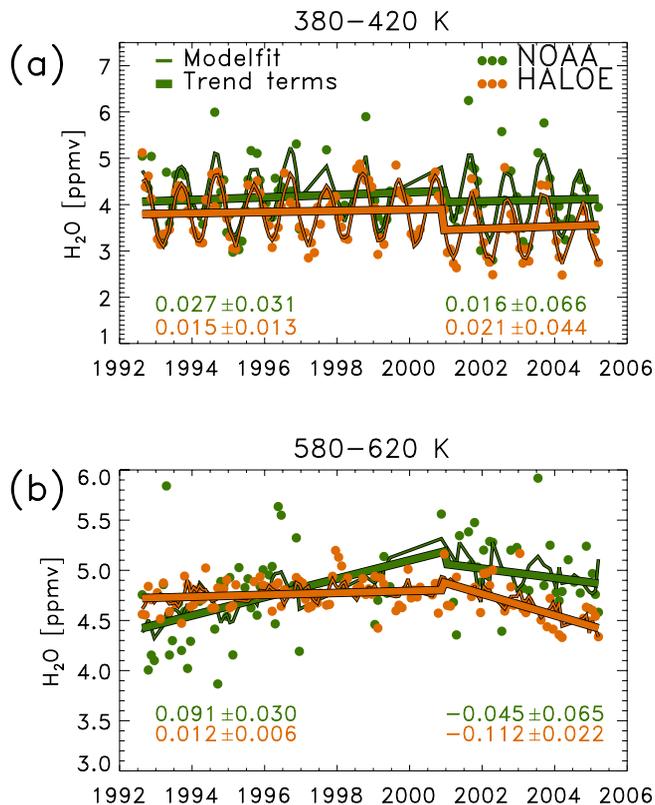
Fig. 6. Observations and regression fit derived from Eq. 5 at **(a)** 380–420 K and **(b)** 580–620 K. Thin lines denote the regression fit and thick lines the trend terms (corresponding to $\mu_1 + \delta\,\mu_2 + \omega_1 X_{1,t} + \omega_2 X_{2,t}$ in Eq. (5). Trend estimates (in ppmv/yr) before and after January 2001 are shown with their 2σ uncertainty in the corresponding colours. Results for NOAA FP are shown for the higher quality data subset.

EGU
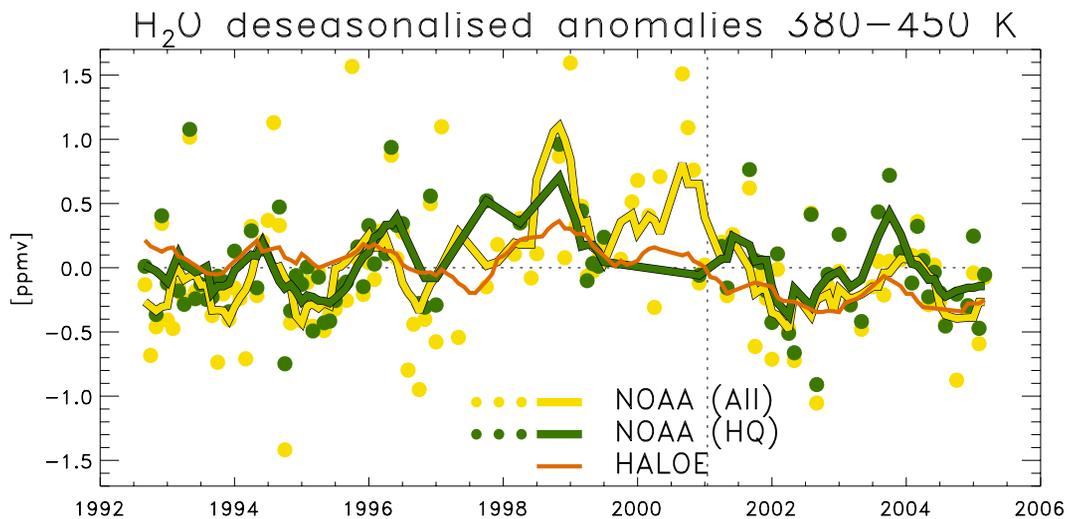
Fig. 7. Deseasonalised anomalies of H$_2$O between 380 and 450 K with a 6 month moving average. For NOAA FP, yellow dots and curve are based on the entire data set; whereas the green dots and line are based on the higher quality soundings only. The moving average of HALOE is shown in orange (no data points). The vertical dotted line indicates January 2001.

EGU
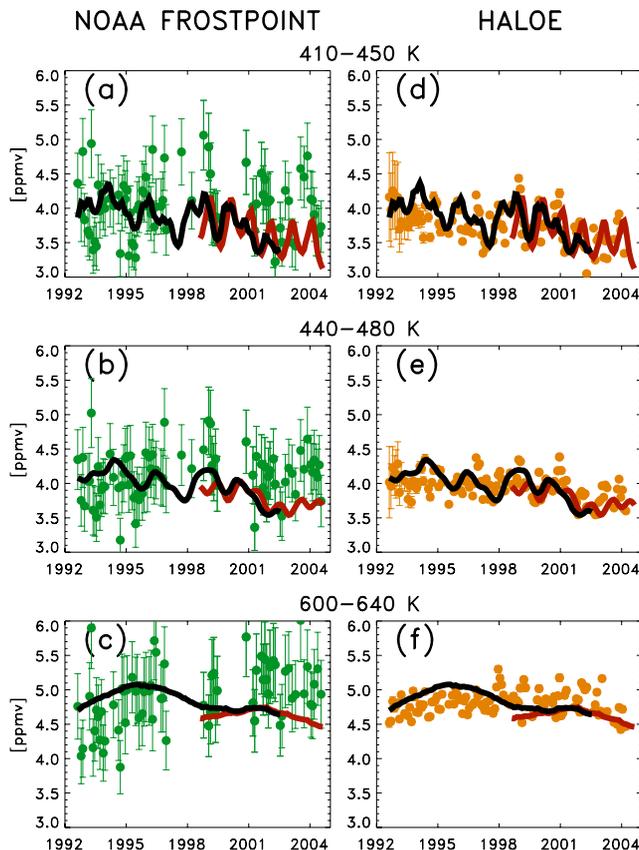
Fig. 8. Observation and model as in Eq. (8) for the layers **(a, d)** 410–450 K, **(b, e)** 440–480 K, **(c, f)** 600–640 K; for NOAA FP (a, b, c) and HALOE (d, e, f). The black line shows a "[H₂O]ₑ-model" estimate and the red line shows a the model estimate using HALOE measurements in the tropics at 400 K (see text). Note that for HALOE, error bars are smaller than the dots, except for low altitudes in the years following the eruption of Mt. Pinatubo.

Title Page

Abstract | Introduction

Conclusions | References

Tables | Figures

|◄ | ►|

◄ | ►

Back | Close

Full Screen / Esc

Printer-friendly Version

Interactive Discussion

EGU
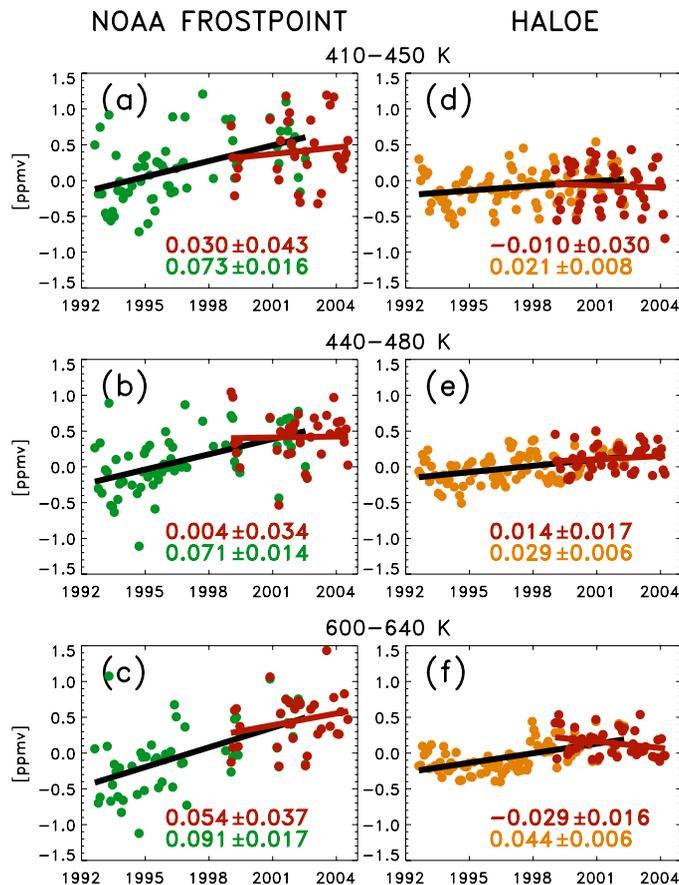
Fig. 9. Residual between model prediction and observations. Figure layout as in Fig. 8. Green: residuals of model results based on $[H_2O]_e$ from Fueglistaler and Haynes (2005); red: residuals of model results based on tropical HALOE measurements at 400 K. Linear trends and 2-σ uncertainty printed in each panel.

Title Page

Abstract　Introduction

Conclusions　References

Tables　Figures

◀　▶

◀　▶

Back　Close

Full Screen / Esc

Printer-friendly Version

Interactive Discussion

EGU